

# Structural and Mechanistic Insights into Methane Oxidation by Particulate Methane Monooxygenase

RAMAKRISHNAN BALASUBRAMANIAN AND  
AMY C. ROSENZWEIG\*

*Departments of Biochemistry, Molecular Biology, and Cell Biology and of Chemistry, Northwestern University, Evanston, Illinois 60208*

Received January 3, 2007

## ABSTRACT

Particulate methane monooxygenase (pMMO) is an integral membrane copper-containing enzyme that converts methane to methanol. Knowledge of how pMMO selectively oxidizes methane under ambient conditions could impact the development of new catalysts. The crystal structure of *Methylococcus capsulatus* (Bath) pMMO reveals the composition and location of three metal centers. Spectroscopic data provide insight into the coordination environments and oxidation states of these metal centers. These results, combined with computational studies and comparisons to relevant systems, are discussed in the context of identifying the most likely site for O<sub>2</sub> activation.

## Introduction

The oxidation of methane to methanol is a challenging reaction because methane is the most inert hydrocarbon (104 kcal mol<sup>-1</sup> C–H bond) and because methanol reacts further at high temperatures.<sup>1</sup> In nature, methanotrophic bacteria oxidize methane to methanol in the first step of their metabolic pathway. Methane hydroxylation is carried out at ambient temperature by methane monooxygenase enzymes (MMOs).<sup>2,3</sup> There are two forms of MMOs. All methanotrophs except members of the *Methylocella* genus produce an integral membrane MMO called particulate methane monooxygenase (pMMO). Several strains also express a cytoplasmic form called soluble methane monooxygenase (sMMO).<sup>2–4</sup> In organisms that possess both forms, including *Methylococcus capsulatus* (Bath) and *Methylosinus trichosporium* OB3b, differential expression is regulated by the bioavailable copper concentration.<sup>5–7</sup> Both MMOs are metalloenzymes, but that is the extent of their similarity. The two systems differ in molecular structure, metal ion composition, and substrate specificity.<sup>8–11</sup>

Ramakrishnan Balasubramanian graduated from the University of Madras with a B.Sc. degree in chemistry in 1995 and from IIT Bombay with a M.Sc. degree in biotechnology in 1997. He received his Ph.D. degree in biochemistry, microbiology, and molecular biology from The Pennsylvania State University in 2006 and is currently a postdoctoral fellow in the laboratory of Amy C. Rosenzweig, studying mechanisms of copper acquisition and utilization in methanotrophs.

Amy C. Rosenzweig graduated from Amherst College in 1988 with a B.A. degree in chemistry and received her Ph.D. degree in inorganic chemistry from MIT in 1994. A 2003 MacArthur Fellow, she is currently Professor of Biochemistry, Molecular Biology, and Cell Biology and Chemistry at Northwestern University. Her research program is focused on structural and biophysical characterization of metalloenzymes and metal-trafficking proteins.

Whereas pMMO is more selective toward alkanes and alkenes that are five carbons or less, substrates for sMMO include alkanes, alkenes, aromatics, and halogenated hydrocarbons.<sup>12,13</sup>

Activation of O<sub>2</sub> by sMMO and related enzymes has been investigated extensively (see the Account by Murray and Lippard in this issue). In contrast, the metal content, organization, and location of the active site in pMMO have been and continue to be controversial. It is only recently that enough information on pMMO has been obtained to begin thinking about O<sub>2</sub> activation chemistry. In the past 5 years, there have been significant advances in the biochemical, spectroscopic, structural, and mechanistic characterization of pMMO. In this Account, we highlight recent discoveries, with an emphasis on their relevance to O<sub>2</sub> activation chemistry.

## Overall Architecture of pMMO

The 2.8 Å resolution crystal structure of *M. capsulatus* (Bath) pMMO revealed its overall architecture for the first time.<sup>14,15</sup> pMMO consists of three subunits, pmoA ( $\beta$ ), pmoB ( $\alpha$ ), and pmoC ( $\gamma$ ), with molecular masses  $\sim$ 24,  $\sim$ 47, and  $\sim$ 22 kDa, respectively. The three subunits assemble into a cylindrical  $\alpha_3\beta_3\gamma_3$  trimeric structure that is  $\sim$ 105 Å in height and  $\sim$ 90 Å in diameter (Figure 1A). The pmoA and pmoC subunits comprise the bulk of the membrane-spanning regions and are composed of seven and five transmembrane helices, respectively. In contrast, pmoB includes two distinct cupredoxin-like  $\beta$  barrels linked by two transmembrane helices and a long loop region. The  $\beta$  barrels from pmoB form a soluble domain that houses two of the three metal centers identified in each protomer in the crystal structure (Figure 1B).

In addition to the crystal structure, Dalton and co-workers determined the structure of *M. capsulatus* (Bath) pMMO by electron microscopy (EM).<sup>16</sup> Although the 23 Å resolution cryo-EM structure limits detailed comparisons with the crystallographic data, two observations are particularly significant. First, the EM structure represents an active complex and agrees well with the overall oligomeric state and architecture of the subunits in the crystal structure. Thus, the crystal structure of pMMO is physiologically relevant. Second, the identification of side “holes” in the soluble regions near the membrane interface are hypothesized to serve as entry points for hydrophobic substrates (Figure 1A). A central cavity, present in both X-ray and EM structures, may function in product egress.<sup>16</sup> Recent cryo-EM studies suggest that the pMMO trimer forms a larger assembly with methanol dehydrogenase (MDH), the subsequent enzyme in the methanotroph metabolic pathway. In the complex, MDH is proposed to interact with the soluble  $\beta$ -barrel regions of pmoB.<sup>17</sup>

\* To whom correspondence should be addressed. E-mail: amyr@northwestern.edu.

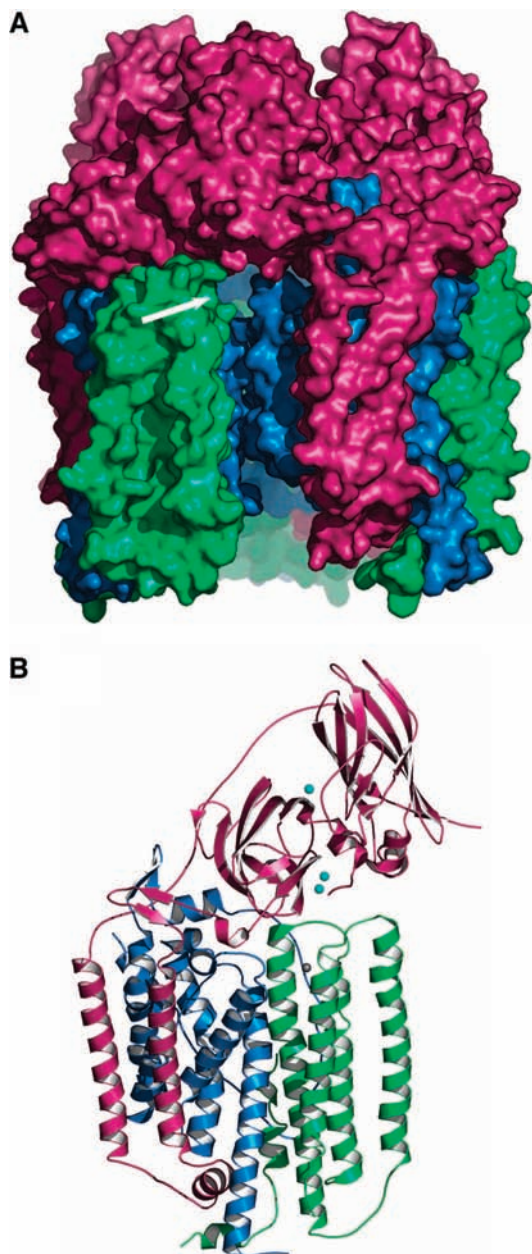


**FIGURE 1.** Structure of pMMO. (A) Surface representation of the trimer. The pmoB subunit is shown in magenta; the pmoA subunit is shown in blue; and the pmoC subunit is shown in green. A side "hole" is marked with the white arrow. (B) Ribbon diagram of one protomer. Copper ions are shown as cyan spheres, and the zinc ion is shown as a gray sphere.

## pMMO Metal Centers

**Metal Ion Composition.** Early analyses of the pMMO metal content suggested that copper is the primary metal involved in methane oxidation.<sup>9</sup> Different groups have reported copper stoichiometries for purified *M. capsulatus* (Bath) pMMO of 2 (Dalton laboratory),<sup>18</sup> 2–3 (our laboratory),<sup>19</sup> 8–10 (DiSpirito laboratory),<sup>20</sup> and 15–20 (Chan laboratory)<sup>21,22</sup> copper ions/100 kDa  $\alpha\beta\gamma$  protomer. Purified pMMO from *M. trichosporium* OB3b contains 2 copper ions/100 kDa.<sup>23</sup> Iron is generally also present with reported stoichiometries of 0.75–2.5 ions/100 kDa.<sup>18–20,24</sup> The varying metal ion content highlights the difficulty in

the isolation and purification of pMMO. The discovery of methanobactin, a siderophore-like, copper-binding molecule associated with some preparations,<sup>25–28</sup> resolves some of the discrepancies, however. The DiSpirito preparation containing 8–10 copper ions actually includes 6–8 molecules of methanobactin and 2 copper ions<sup>20</sup> and is thus consistent with values obtained by us<sup>19</sup> and the Dalton group.<sup>18</sup> Most but not all<sup>20</sup> iron-containing pMMO preparations exhibit spectroscopic features characteristic of heme, suggesting that the iron derives from contaminants in the membrane fractions.<sup>19,29</sup>

**Crystal Structure.** Three metal centers were identified in the crystal structure.<sup>14</sup> A mononuclear copper center is located in the soluble domain of pmoB, ~25 Å from the surface of the membrane. The  $\delta$  nitrogen atoms of His 48 and His 72 coordinate this copper ion. Residue Gln 404, located ~3 Å from this site, might hydrogen bond to coordinated solvent ligands that are not observed at 2.8 Å resolution (Figure 2A). Sequence alignments of pmoB with homologues from other methanotrophs and ammonia-oxidizing bacteria reveal that neither His 48 nor Gln 404 is conserved and that only His 72 is present in most methanotroph pmoB sequences.<sup>8</sup> A dinuclear copper center in pmoB is located ~21 Å from the mononuclear copper site. Residues His 33, His 137, and His 139 together with the amino-terminal nitrogen of His 33 were modeled as ligands to the two copper ions, which are separated by 2.6 Å (Figure 2B). It is likely that yet-to-be-identified exogenous ligands are also present at this site. The ligands to the dinuclear copper site are all strictly conserved.<sup>8</sup> Finally, the crystal structure reveals a zinc ion within the membrane, ~19 Å from the dicopper center and ~32 Å from the mononuclear copper site. This zinc ion is coordinated by His 160, His 173, and Asp 156 from pmoC and Glu 195 from pmoA (Figure 2C). Zinc was used for crystallization but is not associated with purified pMMO<sup>14</sup> and not detected in X-ray absorption spectroscopy (XAS) samples.<sup>29</sup> Thus, this site probably houses a different metal ion in vivo, perhaps a copper ion. A total number of 3–4 copper ions/protomer in the crystal structure is consistent with most earlier metal analyses.<sup>9</sup>

**Spectroscopic Data.** Both membrane-bound and purified pMMO have been studied extensively by spectroscopic techniques. Prior to the crystal structure, these data were used to suggest models for the metal centers.<sup>9,15,30</sup> At this point, we are trying to reconcile these data with the crystal structure to assess the physiological relevance of the structure and to glean more detailed information on the metal coordination environments and oxidation states. Electron paramagnetic resonance (EPR) spectroscopy has been widely used to investigate pMMO. Chan and co-workers report a broad isotropic signal at  $g \sim 2.1$ , which was proposed to derive from a ferromagnetically coupled trinuclear  $\text{Cu}^{\text{II}}$  cluster.<sup>31</sup> Because no trinuclear copper center is present in the structure, alternative interpretations for this signal, such as methanobactin,<sup>24</sup> superposition of a radical signal with a type 2  $\text{Cu}^{\text{II}}$  signal,<sup>32</sup>  $\text{Cu}[\text{Fe}(\text{CN})_6]^{2-}$ ,<sup>33</sup> or adventitiously bound copper ions,<sup>18</sup> might be more reasonable. All researchers observe a type

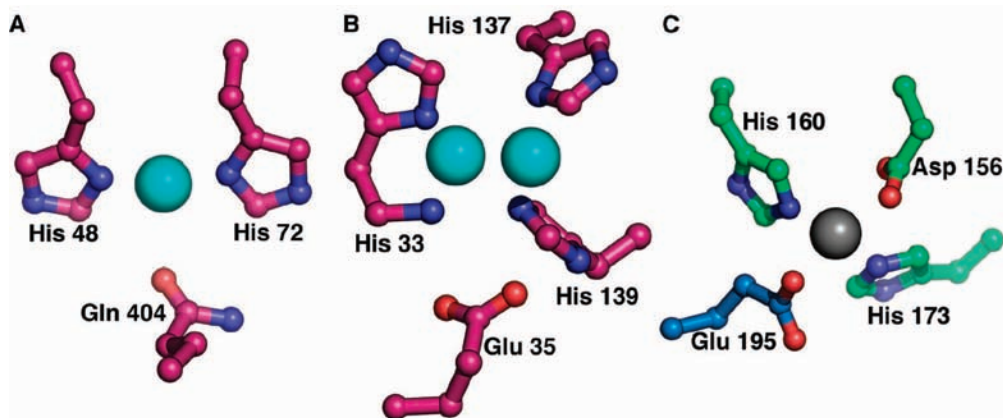


**FIGURE 2.** pMMO metal centers. (A) Mononuclear copper center. (B) Dinuclear copper center. (C) Zinc center. Oxygen atoms are colored red; nitrogen atoms are colored blue; and carbon atoms are colored according to the subunit as in Figure 1B.

	Mononuclear copper site	Dinuclear copper site	"Zinc" site
Scenario 1			
Scenario 2			
Scenario 3			

**FIGURE 3.** Possible scenarios for the oxidation states of the pMMO copper centers based on knowledge from the crystal structure and spectroscopic data.

2 Cu<sup>II</sup> signal for both membrane-bound and purified pMMO.<sup>18–20,24,34,35</sup> This signal accounts for 40–50% of the total copper present, disappears upon chemical reduction,<sup>18,19,29</sup> and is not altered by the addition of azide or cyanide.<sup>35</sup>

The X-ray absorption near edge spectra (XANES) of purified pMMO samples exhibit a feature at 8984 eV, attributable to a Cu<sup>I</sup> 1s → 4p transition.<sup>19</sup> This peak increases in intensity upon chemical reduction with dithionite, indicating that some of the copper ions are present as Cu<sup>II</sup> in purified pMMO. Treatment with H<sub>2</sub>O<sub>2</sub> diminishes this peak, suggesting that some oxidation can occur.<sup>29</sup> Complete oxidation might require turnover in the presence of a substrate.<sup>34</sup> Extended X-ray absorption fine structure (EXAFS) data for purified pMMO are best fit with two Cu–O/N ligand environments, with Cu–O/N distances ranging from 1.93 to 2.22 Å. A second scattering interaction is best fit with a Cu–Cu interaction at 2.51 Å for as-isolated pMMO and 2.65 Å for pMMO reduced with dithionite.<sup>29</sup> This Cu–Cu interaction was critical to our

crystallographic model of the dicopper center because 2.8 Å resolution data cannot necessarily resolve two copper ions at such a close distance. The EXAFS data also support the presence of exogenous ligands because the coordination number of 2–4 for the O/N ligands exceeds the two nitrogen ligands coordinated to each copper ion in the crystal structure. Furthermore, the pMMO EXAFS resembles that of dicopper model compounds, in which the copper ions are four- and five-coordinate.<sup>29</sup>

**Possible Oxidation States.** When the spectroscopic data are taken together with the structure, they suggest several possible schemes for the oxidation states of the pMMO metal centers (Figure 3).<sup>29</sup> We consider these scenarios in the context of three findings: all pMMO samples, including those from *M. trichosporium* OB3b<sup>23</sup> and *M. capsulatus* (strain M),<sup>35</sup> exhibit a type 2 Cu<sup>II</sup> signal that disappears upon reduction, EXAFS data indicate an increase in the Cu–Cu distance upon reduction, and as-isolated pMMO contains a mixture of Cu<sup>I</sup> and Cu<sup>II</sup>. An additional consideration, on the basis of the sequence



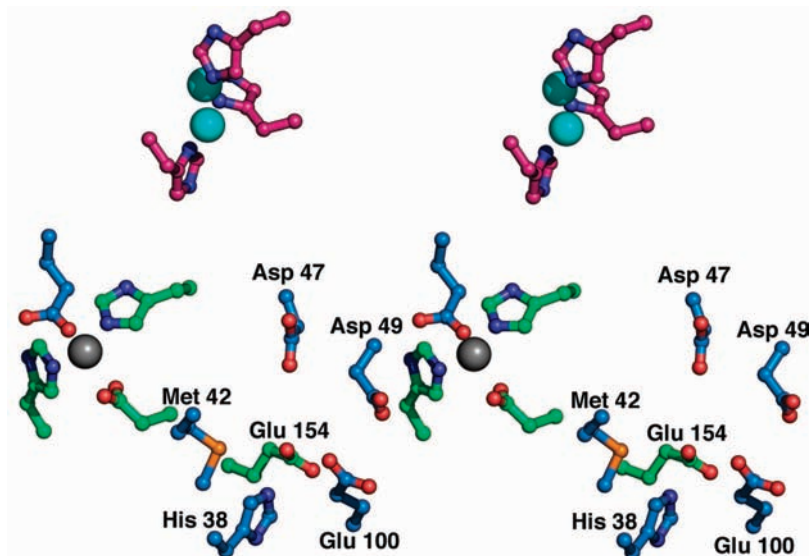


**FIGURE 4.** Stereoview of the dinuclear copper center, the zinc center, and a conserved patch of hydrophilic residues that could form an additional metal-binding site. Only residues in the hydrophilic patch are labeled. Oxygen atoms are colored red; nitrogen atoms are colored blue; sulfur atoms are colored orange; and carbon atoms are colored according to the subunit as in Figure 1B.

conservation of the metal ligands, is that the mononuclear copper center observed in the *M. capsulatus* (Bath) pMMO crystal structure may not be conserved in pMMOs from other methanotrophs.<sup>8</sup> A caveat to this discussion is that, although the EXAFS samples did not photoreduce during data collection, we cannot exclude the possibility of instantaneous photoreduction upon exposure to X-rays, which would complicate a comparison of EPR and EXAFS data.

In the first scenario (scenario 1 in Figure 3), the dicopper center is occupied by EPR silent, antiferromagnetically coupled  $\text{Cu}^{\text{II}}\text{Cu}^{\text{II}}$  and the mononuclear copper site is  $\text{Cu}^{\text{II}}$ , giving rise to the type 2 signal. Upon reduction, the dinuclear site would be converted to  $\text{Cu}^{\text{I}}\text{Cu}^{\text{I}}$ , explaining the increase in the Cu–Cu distance observed by EXAFS. However, the XANES spectra indicate the presence of  $\text{Cu}^{\text{I}}$  in the as-isolated pMMO, which would only be consistent with this model if the zinc site were loaded with  $\text{Cu}^{\text{I}}$ . If the mononuclear copper site is not present in all pMMOs, the spectroscopic data are not compatible with scenario 1. Another possibility (scenario 2 in Figure 3) is that the dicopper site is  $\text{Cu}^{\text{I}}\text{Cu}^{\text{I}}$  and the mononuclear copper site is EPR-active  $\text{Cu}^{\text{II}}$ . The zinc site could be occupied by either  $\text{Cu}^{\text{I}}$  or  $\text{Cu}^{\text{II}}$ . If pMMOs from other organisms have the dicopper and zinc sites and lack the mononuclear copper site, the zinc site would have to be occupied by  $\text{Cu}^{\text{II}}$ . One issue with this scenario is that the increase in the Cu–Cu distance upon reduction would have to be attributed to a change other than redox chemistry. Finally, the dicopper center could be a trapped valence  $\text{Cu}^{\text{I}}\text{Cu}^{\text{II}}$  site (scenario 3 in Figure 3). The type 2 signal would then derive from the dicopper site, and reduction would result in the loss of the EPR signal as well as an increase in the Cu–Cu distance. Copper at the mononuclear and zinc sites could either be  $\text{Cu}^{\text{I}}$  or  $\text{Cu}^{\text{II}}$ . Because site-directed mutagenesis is currently not an option for pMMO, which is obtained directly from methanotrophs<sup>9</sup> rather than from

a heterologous expression system, other methods to distinguish among these scenarios, including spectroscopic and structural characterization of pMMOs from other methanotrophs, must be pursued.

## In Search of the Active Site

**Subunit Localization.** Prior to the crystal structure, experiments using radiolabeled acetylene, a suicide substrate, were used to probe the active-site location. In three different studies, the 24 kDa pmoA subunit was labeled.<sup>24,36,37</sup> Similar studies with the related enzyme ammonia monooxygenase are consistent with this result, with a 28 kDa subunit acquiring the label.<sup>38,39</sup> Some labeling of the 47 kDa pmoB subunit was also observed.<sup>24</sup> The labeling is believed to derive from an activated acetylene intermediate that covalently modifies residues in the active site or nearby.<sup>37</sup> These data thus suggest that the active site is located in the pmoA subunit with perhaps some involvement of pmoB. According to the crystal structure, pmoA is the least involved in metal coordination, contributing only Glu 195 to the zinc site. If the zinc site represents the location of the active site, it is curious that pmoC, which contributes the other three ligands, is not modified. One way to explain the acetylene-labeling results is to consider a cluster of hydrophilic residues in pmoA adjacent to the zinc site (Figure 4).<sup>8,14</sup> These residues, which include His 38, Met 42, Asp 47, Asp 49, and Glu 100 as well as Glu 154 from pmoC, are highly conserved and could conceivably form a metal-binding site that was depleted during purification and/or crystallization. Labeling of pmoB is easier to rationalize because both the mono- and dinuclear copper centers are located within this subunit.

The structural data offer an explanation for why pmoA and pmoB might both be labeled. Dalton and co-workers suggest that the side “holes” observed in the cryo-EM and

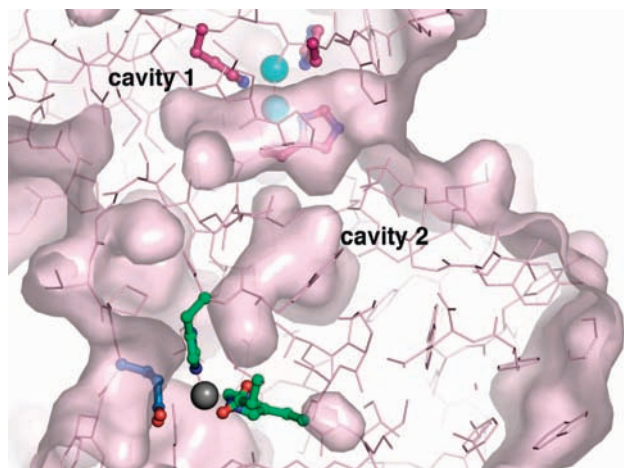


**FIGURE 5.** Cutaway view of the pMMO protein surface near the dinuclear copper and zinc sites showing internal cavities.

crystal structures represent a route for substrate entry.<sup>16</sup> These openings are near the pmoB dicopper center as well as the zinc site and adjacent pmoA hydrophilic cluster. One possibility is that labeled acetylene products diffuse to the two locations, exploiting these “holes”. Diffusion between these sites in pmoB and pmoA may be further enhanced by two adjacent cavities (Figure 5). The first is lined by several conserved hydrophobic residues, including Pro 94 from pmoB and Leu 78, Ile 163, and Val 164 from pmoC. The second includes some of the same residues and extends to the zinc site.<sup>14</sup> Although these observations do not address the exact location of the active site, they do help solve the puzzle of the acetylene labeling data. A corollary to this argument is that the active site probably is not located at the pmoB mononuclear copper center because there is not an obvious path for diffusion of acetylene intermediates from this location to the pmoA subunit.

**Active-Site Identity.** Detailed knowledge of the identity, coordination environment, and oxidation state of the active site is critical to understand how pMMO activates O<sub>2</sub>. There are five possibilities for the active site: the pmoB mononuclear copper center, the pmoC/pmoA zinc center, the pmoB dinuclear copper center, the pmoA hydrophilic cluster, and the trinuclear cluster proposed by Chan and co-workers. At this juncture, the mononuclear copper site in pmoB seems unlikely because all of the ligands to the metal at this site are not conserved.<sup>8</sup> Because no evidence for a trinuclear copper cluster was found in the crystal structure, we will not consider this option either, although methane hydroxylation at such a site has been investigated recently by density functional theory (DFT) calculations.<sup>40</sup> There is currently no evidence for metal binding at the pmoA hydrophilic cluster either. The remaining two options, the pmoC/pmoA zinc center and the pmoB dinuclear copper center, warrant further discussion.

**O<sub>2</sub> Activation at a Mononuclear Copper Center.** Even though the pmoB mononuclear copper site has been discounted, the possibility of O<sub>2</sub> activation at a mononuclear copper center remains if the pmoC/pmoA zinc center contains copper *in vivo*. In considering this site, it

is important to note that the ligands will likely be different from those coordinating zinc in the crystal structure. For example, several potential copper ligands, such as Met 199 from pmoA, are in the vicinity. Binding and activation of O<sub>2</sub> occurs at mononuclear copper centers in the enzymes peptidylglycine  $\alpha$ -hydroxylating monooxygenase (PHM), which hydroxylates the C <sub>$\alpha$</sub>  atom of a terminal glycine residue, and dopamine  $\beta$ -hydroxylase (D $\beta$ M), which converts dopamine to norepinephrine.<sup>41</sup> In PHM, there are two noncoupled mononuclear copper centers, Cu<sub>A</sub> and Cu<sub>B</sub>, that are separated by 11 Å. Substrate and O<sub>2</sub> bind at the Cu<sub>B</sub> site, which is coordinated by two histidines, a methionine, and a solvent molecule.<sup>42</sup> Crystals of PHM soaked with substrate analogues under reducing conditions show electron density at the Cu<sub>B</sub> site that is best modeled as O<sub>2</sub>. Surprisingly, O<sub>2</sub> binds with an end-on  $\eta^1$  geometry, with distances of 2.1 and 2.8 Å from the copper ion to the two oxygen atoms.<sup>43</sup> This crystallographic model is consistent with biochemical and computational data, suggesting that Cu<sup>II</sup>-superoxide is the reactive species,<sup>44–46</sup> as well as with the recent characterization of an end-on  $\eta^1$  superoxo–Cu<sup>II</sup> complex that is able to hydroxylate and hydroperoxylate phenols.<sup>47</sup>

Could a similar species be important in pMMO? One difference is that the C–H bond dissociation energy in methane is 104 kcal/mol as compared to 87 kcal/mol for the PHM substrate.<sup>46</sup> In addition, DFT calculations suggest that Cu<sup>II</sup>-superoxide cannot abstract a hydrogen atom from methane.<sup>48</sup> On the basis of calculations using a model with two imidazoles and one acetate to mimic the pmoB monocopper center, Yoshizawa and Shiota propose a mechanism for methane hydroxylation involving a Cu<sup>III</sup>-oxo reactive species.<sup>48</sup> According to their hypothesis, the initial reaction of Cu<sup>I</sup> with O<sub>2</sub> results in Cu<sup>II</sup>-superoxide, which is converted to Cu<sup>II</sup>-hydroperoxide by hydrogen atom transfer from a tyrosine residue in the active site. Abstraction of a hydrogen atom from a second tyrosine would then yield the Cu<sup>III</sup>-oxo species and a water molecule. The idea that tyrosine residues are involved derives from mechanistic proposals for PHM and D $\beta$ M,<sup>46</sup> which have actually been ruled out by mutagenesis data.<sup>49</sup> Yoshizawa and Shiota invoke participation of specific tyrosine residues near the pmoB mononuclear copper center. Their proposal could be modified to apply to the zinc site because two conserved tyrosines, Tyr 196 from pmoA and Tyr 178 from pmoC, are adjacent. At present, these ideas remain highly speculative.

**O<sub>2</sub> Activation at a Dinuclear Copper Center.** The case for the dicopper center as the active site is stronger than that for a monocopper center for several reasons. First, all of the ligands to this site are highly conserved. Second, the existence of the dicopper center is clear from both EXAFS<sup>29</sup> and crystallographic data.<sup>14</sup> In contrast, the pmoB monocopper center observed in the crystal structure may not be conserved, and the existence of a monocopper center at the crystallographic zinc site has not been established definitively. Third, a bis( $\mu$ -oxo)dicopper core in copper-loaded zeolites has been demonstrated to oxidize methane selectively.<sup>50</sup> Fourth, there is ample

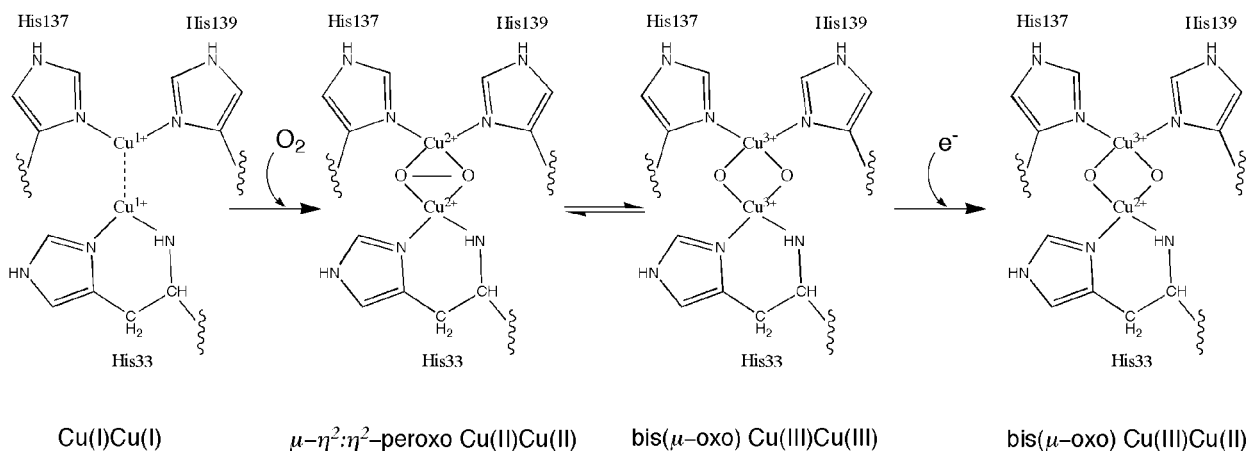


**FIGURE 6.** Possible intermediates for  $\text{O}_2$  activation at the dinuclear copper center.

precedence for  $\text{O}_2$  binding and activation at dinuclear copper centers. In tyrosinase and catechol oxidase, dicopper centers catalyze the hydroxylation of tyrosine and the conversion of catechols to quinones, respectively. The active sites in these enzymes differ from the pMMO dicopper center, in that the two copper ions are ligated by six rather than three histidines and the Cu–Cu distances are longer.<sup>51</sup> In these enzymes, the active species is likely to be a side-on  $\mu\text{-}\eta^2\text{:}\eta^2$  peroxo dicopper(II) complex.<sup>52,53</sup> The isoelectronic species in which the peroxo O–O bond is cleaved to yield a bis( $\mu\text{-oxo}$ )dicopper(III) complex has been characterized in model compounds, although not yet in biology. Interconversion between the bis( $\mu\text{-oxo}$ )dicopper(III) and  $\mu\text{-}\eta^2\text{:}\eta^2$  peroxo dicopper(II) cores has been observed for many synthetic systems and is the subject of several theoretical studies.<sup>54–56</sup>

Could one of these moieties be involved in methane oxidation by pMMO? By analogy to the above enzymes and model complexes,  $\text{O}_2$  could react with a dicopper(I) center in pMMO to yield either a  $\mu\text{-}\eta^2\text{:}\eta^2$  peroxo dicopper(II) or a bis( $\mu\text{-oxo}$ )dicopper(III) species. Injection of an electron might then generate the mixed valent bis( $\mu\text{-oxo}$ ) $\text{Cu}^{\text{II}}\text{Cu}^{\text{III}}$  complex, which has been suggested to be more reactive (Figure 6).<sup>30,57</sup> Yoshizawa and Shiota have investigated this possibility by computational methods.<sup>48,58</sup> Using a dicopper model ligated by three imidazoles and one acetate, their results suggest that the mixed valent species is more reactive than the bis( $\mu\text{-oxo}$ )dicopper(III) species and better suited to activation of the C–H bond in methane. Although the mixed valent species is similar in reactivity to the mononuclear  $\text{Cu}^{\text{III}}\text{-oxo}$  complex, its formation is energetically more favorable.<sup>48</sup> One important caveat to these results is that the assumed starting model may not represent the dinuclear copper center accurately. In particular, residue Glu 35 is modeled as a ligand, although its side-chain oxygen atoms are  $>4 \text{ \AA}$  from the copper ions in the crystallographic model (Figure 2B). In addition, the Cu–Cu distance of 2.65  $\text{\AA}$  in reduced pMMO is significantly shorter than that the  $>4 \text{ \AA}$  Cu–Cu distance observed in reduced catechol oxidase and tyrosinase.<sup>51</sup>

**Catalytic Mechanism.** According to DFT calculations, methane oxidation by the mononuclear  $\text{Cu}^{\text{III}}\text{-oxo}$  species discussed above begins with methane weakly bound to

the monocopper center followed by C–H bond cleavage, formation of a nonradical intermediate, and recombination of OH and  $\text{CH}_3$ . A similar mechanism was computed for the bis( $\mu\text{-oxo}$ ) $\text{Cu}^{\text{II}}\text{Cu}^{\text{III}}$  complex.<sup>48</sup> Chan and co-workers have investigated the pMMO mechanism using *M. capsulatus* (Bath) membrane preparations. Hydroxylation of both chiral ethane<sup>59</sup> and chiral butane<sup>60</sup> proceeds with the retention of the configuration. These data combined with hydrogen/deuterium kinetic isotope effects are consistent with a concerted, nonradical mechanism.<sup>59,60</sup> In other studies, the absence of a carbon kinetic isotope effect for propane oxidation was interpreted as evidence of minimal structural change at the carbon center during transition-state formation in the rate-limiting step.<sup>61</sup>

## Conclusions

Recent structural, biochemical, and spectroscopic data have provided the first steps toward understanding  $\text{O}_2$  activation by pMMO. Although the active site has not yet been identified, the dinuclear copper site in the pmoB subunit or an uncharacterized hydrophilic site within the membrane region is the most likely candidate. Further structural and spectroscopic studies are necessary to elucidate the detailed coordination environments of the metal centers, including the possible presence of exogenous ligands. Parallel investigations of pMMOs from different organisms may also help pinpoint which metal center activates  $\text{O}_2$ . If possible, mutagenesis approaches would be extremely informative. Once the active site is identified, the real quest for understanding the methane hydroxylation mechanism can be initiated.

*This work was supported by the National Institutes of Health Grant GM070473.*

## References

- (1) Periana, R. A.; Bhalla, G.; Tenn, W. J.; Young, K. J. H., III; Liu, X. Y.; Mironov, O.; Jones, C. J.; Ziatdinov, V. R. Perspectives on some challenges and approaches for developing the next generation of selective, low temperature, oxidation catalysts for alkane hydroxylation based on the CH activation reaction. *J. Mol. Catal. A: Chem.* **2004**, *220*, 7–25.



- (2) Dalton, H. The Leeuwenhoek lecture 2000—The natural and unnatural history of methane-oxidizing bacteria. *Philos. Trans. R. Soc. London, Ser. B* **2005**, *360*, 1207–1222.
- (3) Hanson, R. S.; Hanson, T. E. Methanotrophic bacteria. *Microbiol. Rev.* **1996**, *60*, 439–471.
- (4) Dumont, M. G.; Murrell, J. C. Community-level analysis: Key genes of aerobic methane oxidation. *Methods Enzymol.* **2005**, *397*, 413–427.
- (5) Murrell, J. C.; McDonald, I. R.; Gilbert, B. Regulation of expression of methane monooxygenases by copper ions. *Trends Microbiol.* **2000**, *8*, 221–225.
- (6) Prior, S. D.; Dalton, H. The effect of copper ions on membrane content and methane monooxygenase activity in methanol-grown cells of *Methylococcus capsulatus* (Bath). *J. Gen. Microbiol.* **1985**, *131*, 155–163.
- (7) Stanley, S. H.; Prior, S. D.; Leak, D. J.; Dalton, H. Copper stress underlies the fundamental change in intracellular location of methane monooxygenase in methane oxidizing organisms: Studies in batch and continuous cultures. *Biotechnol. Lett.* **1983**, *5*, 487–492.
- (8) Hakemian, A. S.; Rosenzweig, A. C. The biochemistry of methane oxidation. *Ann. Rev. Biochem.* **2007**, *76*, Feb 28, manuscript in press.
- (9) Lieberman, R. L.; Rosenzweig, A. C. Biological methane oxidation: Regulation, biochemistry, and active site structure of particulate methane monooxygenase. *Crit. Rev. Biochem. Mol. Biol.* **2004**, *39*, 147–164.
- (10) Merckx, M.; Kopp, D. A.; Sazinsky, M. H.; Blazyk, J. L.; Müller, J.; Lippard, S. J. Dioxxygen activation and methane hydroxylation by soluble methane monooxygenase: A tale of two irons and three proteins. *Angew. Chem., Int. Ed.* **2001**, *40*, 2782–2807.
- (11) Sazinsky, M. H.; Lippard, S. J. Correlating structure with function in bacterial multicomponent monooxygenases and related diiron proteins. *Acc. Chem. Res.* **2006**, *39*, 558–566.
- (12) Colby, J.; Stirling, D. I.; Dalton, H. The soluble methane monooxygenase of *Methylococcus capsulatus* (Bath). Its ability to oxygenate *n*-alkanes, ethers, and alicyclic, aromatic and heterocyclic compounds. *Biochem. J.* **1977**, *165*, 395–402.
- (13) Burrows, K. J.; Cornish, A.; Scott, D.; Higgins, I. J. Substrate specificities of the soluble and particulate methane monooxygenases of *Methylosinus trichosporium* OB3b. *J. Gen. Microbiol.* **1984**, *130*, 327–3333.
- (14) Lieberman, R. L.; Rosenzweig, A. C. Crystal structure of a membrane-bound metalloenzyme that catalyses the biological oxidation of methane. *Nature* **2005**, *434*, 177–182.
- (15) Lieberman, R. L.; Rosenzweig, A. C. The quest for the particulate methane monooxygenase active site. *J. Chem. Soc., Dalton Trans.* **2005**, *21*, 3390–3396.
- (16) Kitmitto, A.; Myronova, N.; Basu, P.; Dalton, H. Characterization and structural analysis of an active particulate methane monooxygenase trimer from *Methylococcus capsulatus* (Bath). *Biochemistry* **2005**, *44*, 10954–10965.
- (17) Myronova, N.; Kitmitto, A.; Collins, R. F.; Miyaji, A.; Dalton, H. Three-dimensional structure determination of a protein supercomplex that oxidizes methane to formaldehyde in *Methylococcus capsulatus* (Bath). *Biochemistry* **2006**, *45*, 11905–11914.
- (18) Basu, P.; Katterle, B.; Andersson, K. K.; Dalton, H. The membrane-associated form of methane monooxygenase from *Methylococcus capsulatus* (Bath) is a copper/iron protein. *Biochem. J.* **2003**, *369*, 417–427.
- (19) Lieberman, R. L.; Shrestha, D. B.; Doan, P. E.; Hoffman, B. M.; Stemmler, T. L.; Rosenzweig, A. C. Purified particulate methane monooxygenase from *Methylococcus capsulatus* (Bath) is a dimer with both mononuclear copper and a copper-containing cluster. *Proc. Natl. Acad. Sci. U.S.A.* **2003**, *100*, 3820–3825.
- (20) Choi, D. W.; Kunz, R. C.; Boyd, E. S.; Semrau, J. D.; Antholine, W. E.; Han, J. I.; Zahn, J. A.; Boyd, J. M.; de la Mora, A. M.; DiSpirito, A. A. The membrane-associated methane monooxygenase pMMO and pMMO-NADH:quinone oxidoreductase complex from *Methylococcus capsulatus* (Bath). *J. Bacteriol.* **2003**, *185*, 5755–5764.
- (21) Nguyen, H. H.; Elliott, S. J.; Yip, J. H.; Chan, S. I. The particulate methane monooxygenase from *Methylococcus capsulatus* (Bath) is a novel copper-containing three-subunit enzyme. Isolation and characterization. *J. Biol. Chem.* **1998**, *273*, 7957–7966.
- (22) Yu, S. S.-F.; Chen, K. H.-C.; Tseng, M. Y.-H.; Wang, Y.-S.; Tseng, C.-F.; Chen, Y.-J.; Huang, D. S.; Chan, S. I. Production of high-quality particulate methane monooxygenase in high yields from *Methylococcus capsulatus* (Bath) with a hollow-fiber membrane bioreactor. *J. Bacteriol.* **2003**, *185*, 5915–5924.
- (23) Miyaji, A.; Kamachi, T.; Okura, I. Improvement of the purification method for retaining the activity of the particulate methane monooxygenase from *Methylosinus trichosporium* OB3b. *Biotechnol. Lett.* **2002**, *24*, 1883–1887.
- (24) Zahn, J. A.; DiSpirito, A. A. Membrane-associated methane monooxygenase from *Methylococcus capsulatus* (Bath). *J. Bacteriol.* **1996**, *178*, 1018–1029.
- (25) Choi, D. W.; Zea, C. J.; Do, Y. S.; Semrau, J. D.; Antholine, W. E.; Hargrove, M. S.; Pohl, N. L.; Boyd, E. S.; Geesey, G. G.; Hartsel, S. C.; Shafe, P. H.; McEllistrem, M. T.; Kisting, C. J.; Campbell, D.; Rao, V.; de la Mora, A. M.; DiSpirito, A. A. Spectral, kinetic, and thermodynamic properties of Cu(I) and Cu(II) binding by methanobactin from *Methylosinus trichosporium* OB3b. *Biochemistry* **2006**, *45*, 1442–1453.
- (26) Hakemian, A. S.; Tinberg, C. E.; Kondapalli, K. C.; Telser, J.; Hoffman, B. M.; Stemmler, T. L.; Rosenzweig, A. C. The copper chelator methanobactin from *Methylosinus trichosporium* OB3b binds Cu(I). *J. Am. Chem. Soc.* **2005**, *127*, 17142–17143.
- (27) Kim, H. J.; Galeva, N.; Larive, C. K.; Alterman, M.; Graham, D. W. Purification and physical-chemical properties of methanobactin: A chalkophore from *Methylosinus trichosporium* OB3b. *Biochemistry* **2005**, *44*, 5140–5148.
- (28) Kim, H. J.; Graham, D. W.; DiSpirito, A. A.; Alterman, M. A.; Galeva, N.; Larive, C. K.; Asunskis, D.; Sherwood, P. M. A. Methanobactin, a copper-acquisition compound from methane oxidizing bacteria. *Science* **2004**, *305*, 1612–1615.
- (29) Lieberman, R. L.; Kondapalli, K. C.; Shrestha, D. B.; Hakemian, A. S.; Smith, S. M.; Telser, J.; Kuzelka, J.; Gupta, R.; Borovik, A. S.; Lippard, S. J.; Hoffman, B. M.; Rosenzweig, A. C.; Stemmler, T. L. Characterization of the particulate methane monooxygenase metal centers in multiple redox states by X-ray absorption spectroscopy. *Inorg. Chem.* **2006**, *45*, 8372–8381.
- (30) Chan, S. I.; Chen, K. H.-C.; Yu, S. S.-F.; Chen, C.-L.; Kuo, S. S.-J. Toward delineating the structure and function of the particulate methane monooxygenase from methanotrophic bacteria. *Biochemistry* **2004**, *43*, 4421–4430.
- (31) Hung, S.-C.; Chen, C.-L.; Chen, K. H.-C.; Yu, S. S.-F.; Chan, S. I. The catalytic copper clusters of the particulate methane monooxygenase from methanotrophic bacteria: Electron paramagnetic resonance spectral simulations. *J. Chin. Chem. Soc.* **2004**, *51*, 1229–1244.
- (32) Yuan, H.; Collins, M. L. P.; Antholine, W. E. Low-frequency EPR of the copper in particulate methane monooxygenase from *Methylobacterium albus* BG8. *J. Am. Chem. Soc.* **1997**, *119*, 5073–5074.
- (33) Yuan, H.; Collins, M. L. P.; Antholine, W. E. Concentration of Cu, EPR-detectable Cu, and formation of cupric-ferrocyanide in membranes with pMMO. *J. Inorg. Biochem.* **1998**, *72*, 179–185.
- (34) Chen, K. H.-C.; Chen, C.-L.; Tseng, C.-F.; Yu, S. S.-F.; Ke, S.-C.; Lee, J.-F.; Nguyen, H. T.; Elliott, S. J.; Alben, J. O.; Chan, S. I. The copper clusters in the particulate methane monooxygenase (pMMO) from *Methylococcus capsulatus* (Bath). *J. Chin. Chem. Soc.* **2004**, *51*, 1081–1098.
- (35) Katterle, B.; Gvozdev, R. I.; Abudu, N.; Ljones, T.; Andersson, K. K. A continuous-wave electron-nuclear double resonance (X-band) study of the Cu<sup>2+</sup> sites of particulate methane mono-oxygenase of *Methylococcus capsulatus* (strain M) in membrane and pure dopamine  $\beta$ -mono-oxygenase of the adrenal medulla. *Biochem. J.* **2002**, *363*, 677–686.
- (36) Cook, S. A.; Shiemke, A. K. Evidence that copper is a required cofactor for the membrane-bound form of methane monooxygenase. *J. Inorg. Biochem.* **1996**, *63*, 273–284.
- (37) Prior, S. D.; Dalton, H. Acetylene as a suicide substrate and active site probes for methane monooxygenase from *Methylococcus capsulatus* (Bath). *FEMS Microbiol. Lett.* **1985**, *29*, 105–109.
- (38) Hyman, M. R.; Wood, P. M. Suicidal inactivation and labelling of ammonia monooxygenase by acetylene. *Biochem. J.* **1985**, *227*, 719–725.
- (39) Hyman, M. R.; Arp, D. J. <sup>14</sup>C<sub>2</sub>H<sub>2</sub>-Labeling and <sup>14</sup>CO<sub>2</sub>-labeling studies of the de novo synthesis of polypeptides by *Nitrosomonas europaea* during recovery from acetylene and light inactivation of ammonia monooxygenase. *J. Biol. Chem.* **1992**, *267*, 1534–1545.
- (40) Chen, P. P.-Y.; Chan, S. I. Theoretical modeling of the hydroxylation of methane as mediated by the particulate methane monooxygenase. *J. Inorg. Biochem.* **2006**, *100*, 801–809.
- (41) Prigge, S. T.; Mains, R. E.; Eipper, B. A.; Amzel, L. M. New insights into copper monooxygenases and peptide amidation: Structure, mechanism and function. *Cell. Mol. Life Sci.* **2000**, *57*, 1236–1259.
- (42) Prigge, S. T.; Kolhekar, A. S.; Eipper, B. A.; Mains, R. E.; Amzel, L. M. Amidation of bioactive peptides: The structure of peptidylglycine  $\alpha$ -hydroxylating monooxygenase. *Science* **1997**, *278*, 1300–1305.
- (43) Prigge, S. T.; Eipper, B. A.; Mains, R. E.; Amzel, L. M. Dioxxygen binds end-on to mononuclear copper in a precatalytic enzyme complex. *Science* **2004**, *304*, 864–867.
- (44) Chen, P.; Solomon, E. I. Oxygen activation by the noncoupled binuclear copper site in peptidylglycine  $\alpha$ -hydroxylating monooxygenase. Reaction mechanism and role of the noncoupled nature of the active site. *J. Am. Chem. Soc.* **2004**, *126*, 4991–5000.

- (45) Evans, J. P.; Ahn, K.; Klinman, J. P. Evidence that dioxygen and substrate activation are tightly coupled in dopamine- $\beta$ -monooxygenase: Implications for the reactive oxygen species. *J. Biol. Chem.* **2003**, *278*, 49691–49698.
- (46) Klinman, J. P. The copper-enzyme family of dopamine  $\beta$ -monooxygenase and peptidylglycine  $\alpha$ -hydroxylating monooxygenase: Resolving the chemical pathway for substrate hydroxylation. *J. Biol. Chem.* **2007**, *281*, 3013–3016.
- (47) Maiti, D.; Fry, H. C.; Woertink, J. S.; Vance, M. A.; Solomon, E. I.; Karlin, K. D. A 1:1 copper-dioxygen adduct is an end-on bound superoxo copper(II) complex which undergoes oxygenation reactions with phenols. *J. Am. Chem. Soc.* **2007**, *129*, 264–265.
- (48) Yoshizawa, K.; Shiota, Y. Conversion of methane to methanol at the mononuclear and dinuclear copper sites of particulate methane monooxygenase (pMMO): A DFT and QM/MM study. *J. Am. Chem. Soc.* **2006**, *128*, 9873–9881.
- (49) Francisco, W. A.; Blackburn, N. J.; Klinman, J. P. Oxygen and hydrogen isotope effects in an active site tyrosine to phenylalanine mutant of peptidylglycine  $\alpha$ -hydroxylating monooxygenase: Mechanistic implications. *Biochemistry* **2003**, *42*, 1813–1819.
- (50) Groothaert, M. H.; Smeets, P. J.; Sels, B. F.; Jacobs, P. A.; Schoonheydt, R. A. Selective oxidation of methane by the bis( $\mu$ -oxo)dicopper core stabilized on ZSM-5 and mordenite zeolites. *J. Am. Chem. Soc.* **2005**, *127*, 1394–1395.
- (51) Rosenzweig, A. C.; Sazinsky, M. H. Structural insights into dioxygen-activating copper enzymes. *Curr. Opin. Struct. Biol.* **2007**, *16*, 729–735.
- (52) Gerdemann, C.; Eicken, C.; Krebs, B. The crystal structure of catechol oxidase: New insight into the function of type-3 copper proteins. *Acc. Chem. Res.* **2002**, *35*, 183–191.
- (53) Solomon, E. I.; Sundaram, U. M.; Machonkin, T. E. Multicopper oxidases and oxygenases. *Chem. Rev.* **1996**, *96*, 2563–2605.
- (54) Hatcher, L. Q.; Karlin, K. D. Oxidant types in copper-dioxygen chemistry: The ligand coordination defines the Cu<sub>n</sub>-O<sub>2</sub> structure and subsequent reactivity. *J. Biol. Inorg. Chem.* **2004**, *9*, 669–683.
- (55) Lewis, E. A.; Tolman, W. B. Reactivity of dioxygen-copper systems. *Chem. Rev.* **2004**, *104*, 1047–1076.
- (56) Mirica, L. M.; Ottenwaelter, X.; Stack, T. D. P. Structure and spectroscopy of copper-dioxygen complexes. *Chem. Rev.* **2004**, *104*, 1013–1045.
- (57) Elliott, S. J.; Zhu, M.; Tso, L.; Nguyen, H.-H.; Yip, J. H.-K.; Chan, S. I. Regio- and stereoselectivity of particulate methane monooxygenase from *Methylococcus capsulatus* (Bath). *J. Am. Chem. Soc.* **1997**, *119*, 9949–9955.
- (58) Yoshizawa, K.; Suzuki, A.; Shiota, Y.; Yamabe, T. Conversion of methane to methanol on diiron and dicopper enzyme models of methane monooxygenase: A theoretical study on a concerted reaction pathway. *Bull. Chem. Soc. Jpn.* **2000**, *73*, 815–827.
- (59) Wilkinson, B.; Zhu, M.; Priestley, N. D.; Nguyen, H.-H. T.; Morimoto, H.; Williams, P. G.; Chan, S. I.; Floss, H. G. A concerted mechanism for ethane hydroxylation by the particulate methane monooxygenase from *Methylococcus capsulatus* (Bath). *J. Am. Chem. Soc.* **1996**, *118*, 921–922.
- (60) Yu, S. S.-F.; Wu, L.-Y.; Chen, K. H.-C.; Luo, W.-I.; Huang, D.-S.; Chan, S. I. The stereospecific hydroxylation of [2,2-<sup>2</sup>H<sub>2</sub>] butane and chiral dideuteriobutanes by the particulate methane monooxygenase from *Methylococcus capsulatus* (Bath). *J. Biol. Chem.* **2003**, *278*, 40658–40669.
- (61) Huang, D. S.; Wu, S. H.; Wang, Y. S.; Yu, S. S.; Chan, S. I. Determination of the carbon kinetic isotope effects on propane hydroxylation mediated by the methane monooxygenases from *Methylococcus capsulatus* (Bath) by using stable carbon isotopic analysis. *ChemBioChem* **2002**, *3*, 760–765.

AR700004S